ACS APPLIED MATERIALS & INTERFACES

Research Article

www.acsami.org

Functionalization of DNA-Dendron Supramolecular Fibers and Application in Regulation of *Escherichia coli* Association

Fen Wu,[†] Juan Jin,[‡] Liying Wang,[†] Pengfei Sun,[§] Huanxiang Yuan,[∥] Zhongqiang Yang,[‡] Guosong Chen,[§] Qing-Hua Fan,*[,†] and Dongsheng Liu*[,‡]

[†]Beijing National Laboratory for Molecular Sciences, CAS Key Laboratory of Molecular Recognition and Function, Institute of Chemistry, Chinese Academy of Sciences (CAS), Beijing 100190, China

[‡]Key Laboratory of Organic Optoelectronics & Molecular Engineering of the Ministry of Education, Department of Chemistry, Tsinghua University, Beijing 100084, China

[§]The State Key Laboratory of Molecular Engineering of Polymers and Department of Macromolecular Science, Fudan University, Shanghai 200433, China

[∥]Beijing National Laboratory for Molecular Sciences (BNLMS), Key Laboratory of Organic Solids, Institute of Chemistry, Chinese Academy of Sciences (CAS), Beijing 100190, China

Supporting Information

ABSTRACT: Specific carbohydrate recognition in biology is a dynamic process. Thus, supramolecular multivalent scaffolds with dynamic features have been applied to mimic this process. Herein, we prepared DNA-dendron supramolecular fibers and synthesized carbohydrate-oligonucleotide conjugates (C18-mannose). Via DNA hybridization, the C18-mannose could be guided onto the fiber platform and form multiple mannose-functionalized fibers, which can be utilized to agglutinate *E. coli* because of high affinity among multivalent mannose ligands and receptors on *E. coli*. In addition, via chain exchange reaction of DNAs, the *E. coli* could be dissociated by replacing multivalent mannose ligands with competitive unmodified DNA sequences. The association and dissociation processes of *E. coli* are confirmed by fluorescent microscope and transmission electron microscope (TEM). These results not only demonstrate the ability of DNA-dendron fibers in reversibly associating *E. coli* but also illustrate their potential to be an easily modified multivalent supramolecular platform.

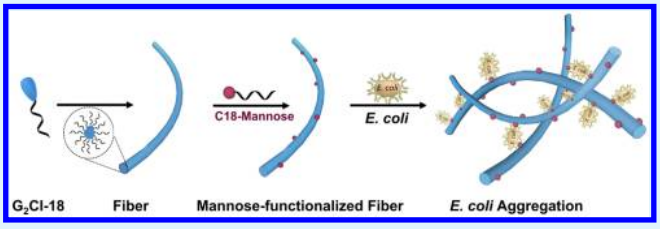

KEYWORDS: *carbohydrate recognition, DNA, self-assembly, multivalent scaffolds, E. coli, association and dissociation*

1. INTRODUCTION

Carbohydrate recognition based on multiple simultaneous interactions among ligands and receptors plays a significant role in mediating interactions between cells and other elements in biology.[1−3] Pathogens can infect cells via specifically binding with carbohydrate on cell surfaces.[4,5] As a consequence, specific recognition between pathogen and cells can be utilized to block their attachments with polyvalent inhibitors. In recent years, synthetic multivalent inhibitors have been explored to prevent undesired biological interactions.[6−17] However, the recognition interaction in biology is a dynamic process; supramolecular systems with dynamic feature have been utilized to mimic this process.[18−22] Recently, owing to designable DNA sequence and hybridization properties, DNA self-assembly has been a trend to provide controllable frames.[23−26] Especially the self-assembly of amphiphilic DNA organic hybrids has been extensively studied, and they could self-assemble into micelles, vesicles, and fibers.[27−33] Herein, we employed DNA-dendron supramolecular fibers with DNA exposed at the corona of fibers. Via DNA hybridization, the carbohydrate ligands could be easily introduced to form a multivalent carbohydrate-functionalized scaffold. This scaffold is able to regulate the association and disassociation of *E. coli*.

Our strategy is illustrated in Scheme 1. We employed fibers assembled from hybrids of poly(benzyl ether) dendron (G_2Cl, where 2 represents the generation of the dendron) and DNA as the basic scaffold.[30] Owing to repulsive interaction of DNA negative charge, DNA strands are well stretched out at the corona of fibers, which facilitates the hybridization of modified complementary DNA. Then, via DNA hybridization, the synthesized carbohydrate-oligonucleotide conjugates (C18-mannose) were loaded onto the corona of fibers to form multivalent mannose-functionalized fibers. Finally, these fibers were utilized as multivalent scaffolds to agglutinate *E. coli*. In addition, via chain exchange reaction of DNAs, the *E. coli* could be dissociated by replacing multivalent mannose ligands with competitive unmodified DNA sequences.

Received: January 23, 2015
Accepted: March 18, 2015
Published: March 18, 2015

DOI: 10.1021/acsami.5b00702
ACS Appl. Mater. Interfaces 2015, 7, 7351−7356

Scheme 1. Illustration of Functionalization of DNA-Dendron Supramolecular Fibers and Regulation of *E. coli* Association

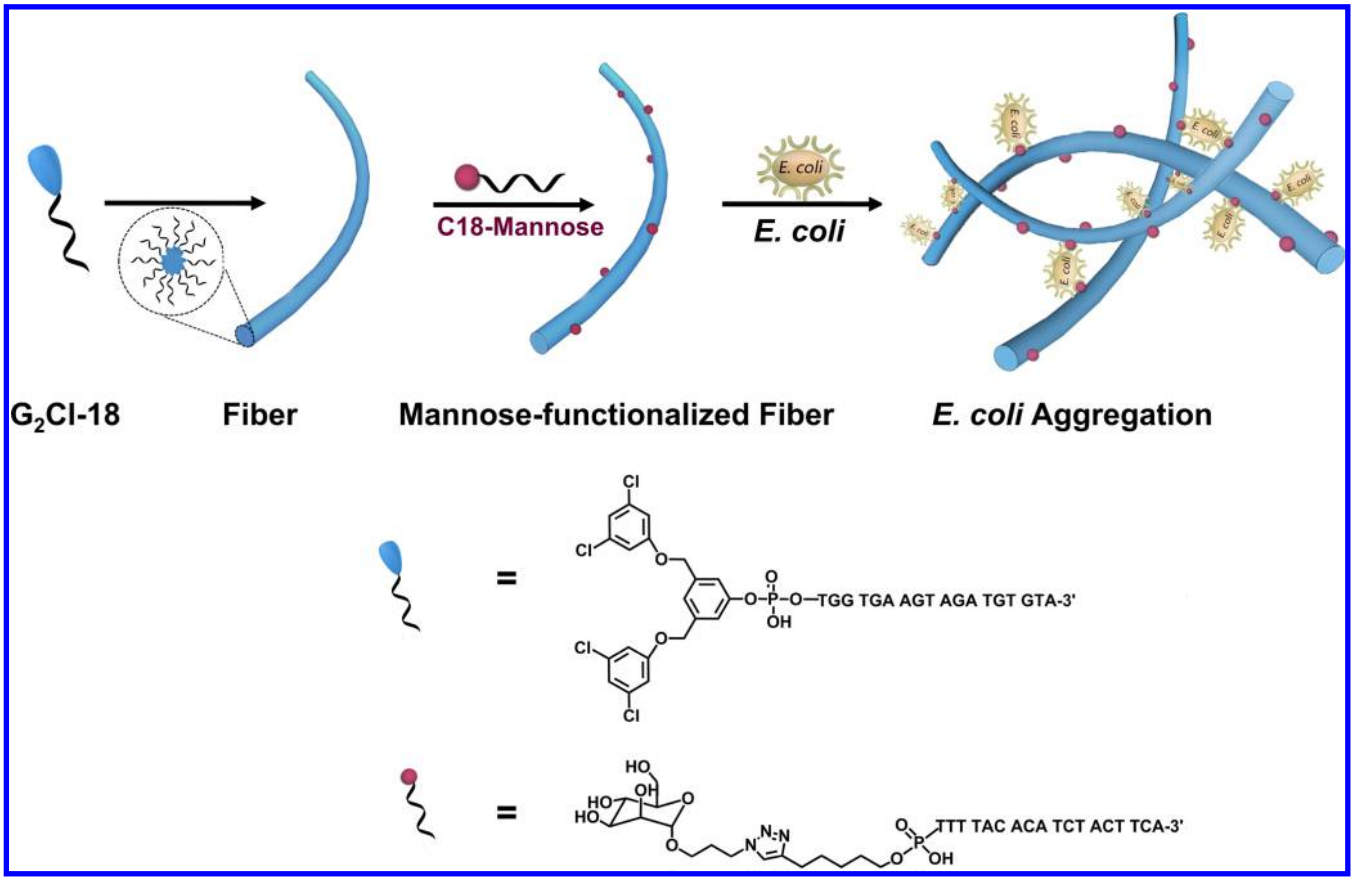

2. EXPERIMENTAL SECTION

2.1. Materials. Chemicals were obtained from Aldrich or Alfa Aesar (Tianjin, China) and used without further treatment unless particularly mentioned. All oligonucleotides were synthesized using ABI 34 DNA synthesizer with a standard phosphoramidite DNA synthesis protocol and purified by reverse high-performance liquid chromatography (HPLC). *E. coli* stains ORN178 and ORN208 were provided from Prof. G. S. Chen in Fudan University. The two stains differ in the properties of mannose binding.

2.2. Synthesis of Carbohydrate-Oligonucleotide Conjugates (C18-Mannose). In a vial, Tris-HCl (1 M, 32 μL), $CuSO_4$ (100 mM, 14 μL), alkynyl-modified oligonucleotide (1 mM, 40 μL), and 3-azidopropyl-α-D-mannopyranoside (1.5 mM, 40 μL) were added in order and then vibrated for 20 s. After NaASc (1 M, 4 μL) was transferred into the vial, the mixture in the aqueous phase was vibrated for 20 s and put in the Thermomixer (room temperature (RT), 12 h, 1500 rpm). The mixture was washed with Tris-borate-EDTA (TBE) and purified by HPLC.

2.3. Preparation of Multivalent Mannose-Functionalized Fibers. The G_2Cl-18 stock solution (20 μM, 100 μL) was added to dichloromethane (DCM) (5 μL). After centrifugation at 6000 rpm for 2 min, the solution was heated to 90 °C and kept for 30 min, then naturally cooled to RT and kept overnight. C18-mannose with different concentrations was added to 50 μL of preformed G_2Cl-18 fiber stock solution (20 μM) overnight (RT).[30]

2.4. Association Experiments of Mannose-Functionalized Fibers with *E. coli*. Four μL of frozen culture of *E. coli* stains was incubated in 10 mL of LB media in a shaker at 37 °C to an optical density of 1.0 at 600 nm. Two hundred μL of culture was precipitated by centrifugation for 5 min at 5000 rpm, and supernatant was removed. The pellet was washed twice with 200 μL of phosphate-buffered saline (PBS, pH 7.2) and redissolved in 200 μL of PBS (pH 7.2, 0.2 mM $CaCl_2$, 0.2 mM $MnCl_2$). The 100 μL of mannose-functionalized fiber stock solution was incubated with the above slurry (RT, 1 h).[21] In contrast, nonfunctionalized fibers or monovalent C18-mannose were incubated with the above slurry. The final mixture was washed with PBS buffer twice, resuspended in 50 μL of PBS buffer, stained with Syto9 (1 μL, 0.5 mM), and shaken (RT, 0.5 h). This suspension was evaluated with a fluorescent microscope (Nikon, Ti–S) using 40× objectives and a transmission electron microscope (TEM, Hitachi HT7700).

2.5. Dissociation Experiments. At the molar ratio of C18-mannose/C18′ = 1:250, 10 μL of the complete complementary DNA C18′ (1 mM) was transferred into 10 μL of the above slurry of *E. coli* association (G_2Cl-18/C18-mannose = 1:0.2), and then the mixture reacted at 25 °C for 2 h with shaking. Then fluorescence observation was performed as above.

3. RESULTS AND DISCUSSION

3.1. Synthesis of C18-Mannose. First, we designed the synthetic route of carbohydrate-oligonucleotide conjugates C18-mannose according to the reported methods.[34−36] The synthetic route was outlined in Scheme S1, Supporting Information. 3-Azidopropyl 2,3,4,6-hydroxy-α-D-mannopyranoside was synthesized and characterized by ^{1}H NMR, ^{13}C NMR, and matrix-assisted laser desorption/ionization–time of flight (MALDI-TOF) (Figure S4, Supporting Information). The alkynyl-functionalized oligonucleotide (C18:5′-TTTTACA-CATCTACTTCA-3′) was synthesized via a typical solid-phase synthesis method,[30−33,37,38] purified by HPLC and characterized by MALDI-TOF. The C18-mannose was synthesized through the copper(I)-catalyzed alkyne–azide 1,3-dipolar cycloaddition (CuAAC) reaction and monitored by polyacrylamide gel electrophoresis (PAGE) (Figure 1a). The lane of product (C18-mannose) ran slower than that of the starting material (C18–N_3), because mannose was attached to

DOI: 10.1021/acsami.5b00702
ACS Appl. Mater. Interfaces 2015, 7, 7351−7356

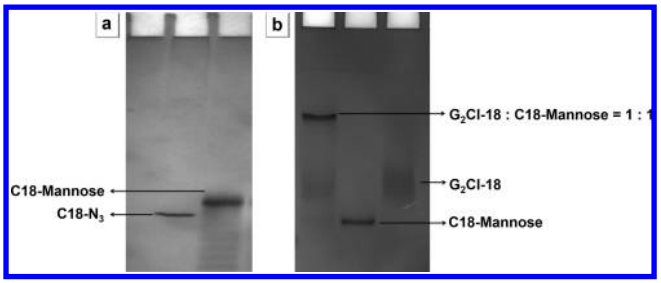

Figure 1. Polyacrylamide gel electrophoresis characterization of (a) C18-mannose and (b) hybridization of G2Cl-18/C18-mannose = 1:1.

DNA and decreased the mobility of the product. In addition, there was just one clear product lane without starting material, indicating mannose was attached with DNA and the yield was almost 100%. After 10% denaturing PAGE purification, the structure of C18-mannose was characterized by MALDI-TOF (Figure S7, Supporting Information). It was a single peak, and the found molecular weight (5813 g/mol) agreed well with the calculated value (5830 g/mol), which further verified the purity of C18-mannose. According to the above results, we have successfully synthesized carbohydrate-oligonucleotide conjugate C18-mannose with a high yield.

3.2. DNA Hybridization between G_2Cl-18 and C18-Mannose. With C18-mannose in hand, the hybridization between C18-mannose (C18:5′-TTTTACACATCTACTTCA-3′) and G_2Cl-18 (18:5′-TGGTGAAGTAGATGTG TA-3′) was conducted and characterized by native PAGE. As shown in Figure 1b, after hybridization there was only a single band and it ran slower than any single-stranded DNA owing to the charge and size interaction, indicating that C18-mannose fully paired with G_2Cl-18.

3.3. Self-Assembly Behavior of G_2Cl-18 and C18-Mannose. After verifying hybridization of G_2Cl-18 and C18-mannose, we investigated the self-assembly behavior of G_2Cl-18 and C18-mannose via TEM and fluorescent microscope. As shown in Figure 2a, the G_2Cl-18 hybrid in the aqueous phase assembled to fibers as confirmed by TEM. The fibers existed exclusively with length of tens of microns and average diameter of 16 nm in TEM images, consistent with the calculated diameter of 18.4 nm.[30] After preformed fibers hybridized with C18-mannose overnight, the morphology and size of mannose-functionalized fibers almost did not change (Figure 2b). Ten μL of Nile Red (38.6 μM) in acetone was added to the above solution overnight to load the fluorescent molecule. Owing to the capacity of hydrophobic fluorescent molecule Nile Red in the hydrophobic core, the fibers showed red fluorescence as confirmed by fluorescent microscope (Figure S8, Supporting Information). The length of red fibers was consistent with that in the TEM images.

3.4. Association Performance of Multivalent Mannose-Functionalized Fibers with *E. coli*. To investigate the multivalent effect of mannose-functionalized fibers to bind with *E. coli* for inhibiting the mobility of *E. coli*, association experiments were carried out on the mannose-functionalized fibers, nonfunctionalized fibers, and monovalent C18-mannose, respectively. The preformed G_2Cl-18 fibers were cultured with C18-mannose overnight for functionalization of fibers. The total concentration of G_2Cl-18 was 20 μM, and C18-mannose was kept at 20 and 4 μM, respectively. These systems were incubated with *E. coli* for 1 h at room temperature, then the slurry was centrifuged to remove the upper liquid and resuspended in PBS buffer, then stained with Syto9 (0.5 mM), and finally evaluated with fluorescent microscope using a 40× objective. As shown in Figure 3, green fluorescence and red fluorescence showed the position of *E. coli* stains ORN178 and fibers, respectively. Clusters of green fluorescent *E. coli* stains ORN178 were observed when they were incubated with mannose-functionalized fibers at the molar ratio of G_2Cl-18/C18-mannose = 1:1 (Figure 3, 1b). The red mannose-functionalized fibers had a good correspondence with green *E. coli* stains ORN178 clusters (Figure 3, 1c). In addition, upon decreasing the ratio of C18-mannose to 0.2, we can still observe the association of *E. coli* stains ORN178 (Figure 3, 2b and 2c). These results indicated that the mannose-functionalized fibers have strong affinity with *E. coli* stains ORN178, and the concentration of C18-mannose had no visible effect on the association of *E. coli*, because the fibers are very long and present enough recognition sites, and the interaction between bacteria and the fiber is multivalent. We proposed that all these factors together make the association not very sensitive to the mannose density on the fiber. Meanwhile, no clusters of green fluorescent *E. coli* stains ORN178 were observed when *E. coli* stains ORN178 were incubated with monovalent C18-mannose (Figure 3, 3b) or nonfunctionalized fibers (Figure 3, 4b). These results indicated that multivalent mannose-functionalized fibers played a significant role in *E. coli* association. The association was due to the recognition between multivalent mannose ligands on the fibers and the receptors on *E. coli*. It also proved

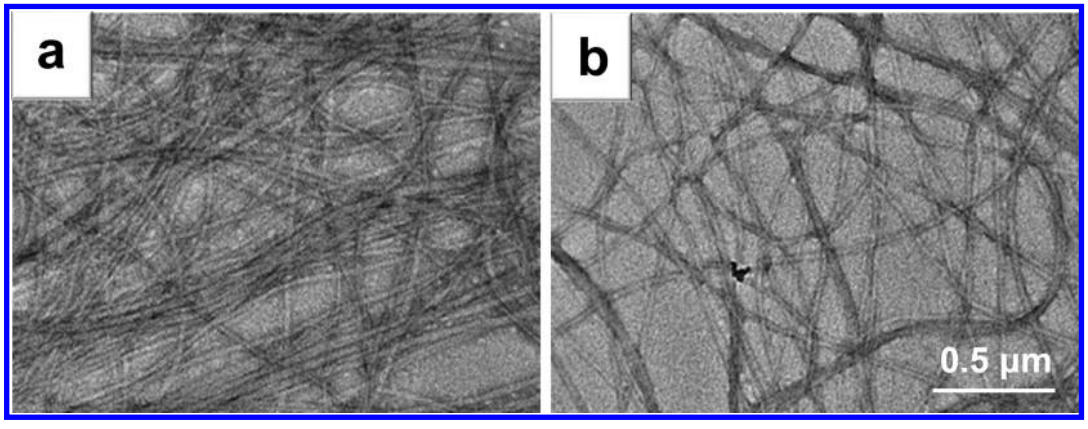

Figure 2. Self-assembly behavior of G_2Cl-18 and C18-mannose. TEM images of (a) fibers of G_2Cl-18 and (b) mannose-functionalized fibers of G_2Cl-18/C18-mannose = 1:0.2 (molar ratio).

DOI: 10.1021/acsami.5b00702
ACS Appl. Mater. Interfaces 2015, 7, 7351−7356

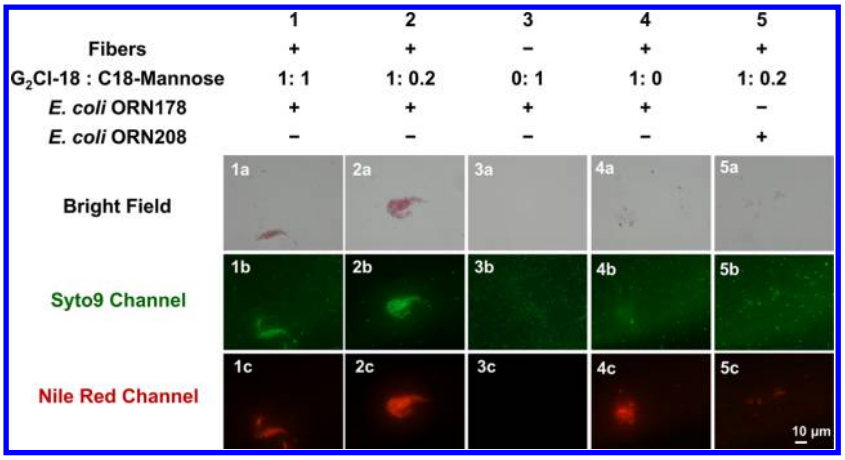

Figure 3. Association performance of mannose-functionalized fibers with *E. coli* strains ORN178 and ORN208. Microscopy pictures in (a) bright field, (b) fluorescence (λex = 485 nm, λem = 498 nm), and (c) fluorescence (λex = 549 nm, λem = 628 nm) mode on ORN178 incubation with (1) 1:1, (2) 1:0.2 G_2Cl-18/C18-mannose, (3) 100% C18-mannose, (4) 100% G_2Cl-18, and on ORN208 incubation with (5) 1:0.2 G_2Cl-18/C18-mannose.

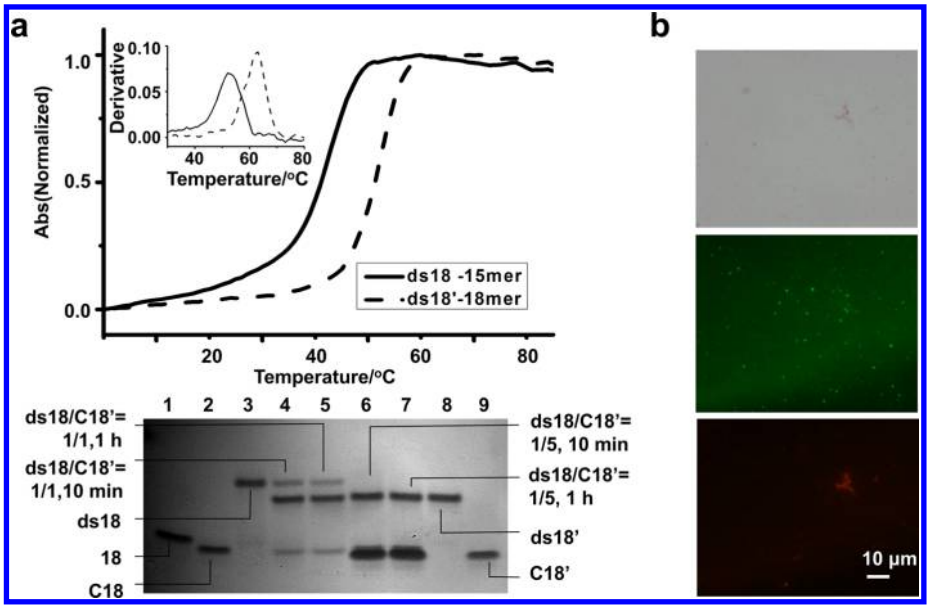

Figure 4. Dissociation performance of *E. coli* strains ORN178 via replacing C18-mannose by removing C18-mannose by DNA displacement reaction. (a) T_m measurements of ds18 and ds18′ and 10% native PAGE characterization of ds18 replaced by C18′. UV melting experiments for UV absorption at 260 nm were carried out from 10 to 95 °C at a rate of 1 °C/min. The concentration of a single DNA strand was 2 μM each. (b) Microscopy pictures in (1) bright field, (2) fluorescence (λex = 485 nm, λem = 498 nm), and (3) fluorescence (λex = 549 nm, λem = 628 nm) mode on the system of C18-mannose/C18′ = 1:250 for G_2Cl-18/C18-mannose = 1:0.2 mannose-functionalized fibers.

that the agglutination ability of multivalent mannose-functionalized fibers was much higher than monovalent C18-mannose and excluded the nonspecific interactions between the self-assembled fibers and *E. coli*.

To investigate the specific interaction of mannose-functionalized fibers with FimH receptors on the *E. coli* strains ORN178, the mannose-functionalized fibers were incubated with control group ORN208, which just differs in the ability to bind with mannose. No clusters of green fluorescent *E. coli* stains ORN208 were observed (Figure 3, 5b); therefore, it proved that the association of mannose-functionalized fibers and ORN178 is induced by the interaction of mannose and FimH receptor, not nonspecific interaction.

We further utilized TEM to investigate the *E. coli* association. The mannose-functionalized fibers were incubated with *E. coli* strains ORN178. The total concentration of G_2Cl-18 was 20 μM, and C18-mannose was kept at 4 μM. As shown in Figure S9, Supporting Information, a few *E. coli* strains ORN178 agglutinated together with the mannose-functionalized fibers because of the recognition and affinity interaction between multivalent mannose ligands on the fibers and receptors on *E. coli* strains ORN178. The TEM results provided further evidence that *E. coli* strains ORN178 association was induced by the multivalent ligands on the scaffolds.

3.5. Dissociation Performance of *E. coli* Strains ORN178. To further study the multivalent influence of mannose-functionalized fibers on the *E. coli* association, an *E. coli* dissociation experiment was carried out via replacing C18-mannose with another fully complementary DNA strand C18′. The complete complementary DNA strands C18′ could hybridize with G_2Cl-18 and replace partial complementary DNA C18-mannose. The complete complementary double-

DOI: 10.1021/acsami.5b00702
ACS Appl. Mater. Interfaces 2015, 7, 7351−7356

stranded DNA ds18′ have 18 base pairs, while the partial complementary double-stranded DNA ds18 have 15 base pairs; consequently, the melting point of double-stranded DNA ds18′ (63 °C) is higher than that of double-stranded DNA ds18 (52 °C). After C18′ replaces C18-mannose, multivalent ligands are changed to monovalent ligand. The break of the multivalent ligands structure will lead to *E. coli* dissociation. As shown in Figure 4a, DNA strands C18′ can replace C18 in 10 min at a molar ratio of C18′/C18 = 5:1. In the system of G_2Cl-18/C18-mannose = 1:0.2, *E. coli* strains ORN178 agglutinated first. Then the slurry was incubated at 25 °C for 2 h with gentle shaking after adding C18′ at the molar ratio of C18-mannose/C18′ = 1:250. As shown in Figure 4b, the *E. coli* strains ORN178 dissociated and dispersed alone. The results not only provided further evidence that the association is owing to the specific binding between *E. coli* strains ORN178 and mannose on the fibers, but also indicated that we can regulate *E. coli* association and dissociation via DNA displacement reaction.

4. CONCLUSIONS

In summary, we have designed a supramolecular multivalent carbohydrate-functionalized scaffold to mimic dynamic arrangements of ligands on cell surfaces. We employed fibers assembled from DNA-dendron hybrids with the hydrophilic DNA shell and the hydrophobic dendron core. The agglutination ability of mannose-functionalized fibers was much higher than monovalent C18-mannose as confirmed by fluorescent microscope and TEM. Utilizing designable DNA sequence and hybridization properties, we can control association and dissociation of *E. coli*. Our results not only demonstrate the ability of DNA-dendron fibers in reversibly associating *E. coli* but also illustrate their potential to be an easily modified multivalent supramolecular platform. It will provide a new strategy for inducing or inhibiting infection to host cells, and this system can be utilized to largely introduce different functional groups[39,40] via DNA hybridization and provides a model system to investigate prevention of cell infection and their potential practical use.

■ ASSOCIATED CONTENT

Supporting Information

The synthetic route of C18-mannose, ^{1}H NMR and ^{13}C NMR MALDI-TOF of mannose derivative, the fluorescent characterization of mannose-functionalized fibers, and TEM characterization of performance of mannose-functionalized fibers with *E. coli* strains ORN178. This material is available free of charge via the Internet at http://pubs.acs.org.

■ AUTHOR INFORMATION

Corresponding Authors

*E-mail: fanqh@iccas.ac.cn.
*E-mail: liudongsheng@tsinghua.edu.cn.

Notes

The authors declare no competing financial interest.

■ ACKNOWLEDGMENTS

We thank Prof. S. Wang at ICCAS for providing cell culture facilities. We thank the National Basic Research Program of China (973 program, no. 2013CB932800), the National Natural Science Foundation of China (no. 91427302, 21421064), NSFC-DFG joint project TRR61, and Beijing Municipal Science &Technology Commission for financial support.

■ REFERENCES

(1) Lee, Y. C.; Lee, R. T. Carbohydrate−Protein Interactions: Basis of Glycobiology. *Acc. Chem. Res.* **1995**, *28*, 321−327.
(2) Dwek, R. A. Glycobiology: Toward Understanding the Function of Sugars. *Chem. Rev.* **1996**, *96*, 683−720.
(3) Mammen, M.; Choi, S.-K.; Whitesides, G. M. Polyvalent Interactions in Biological Systems: Implications for Design and Use of Multivalent Ligands and Inhibitors. *Angew. Chem., Int. Ed.* **1998**, *37*, 2754−2794.
(4) Rudd, P. M. Glycosylation and the Immune System. *Science* **2001**, *291*, 2370−2376.
(5) van Kooyk, Y.; Rabinovich, G. A. Protein-Glycan Interactions in the Control of Innate and Adaptive Immune Responses. *Nat. Immunol.* **2008**, *9*, 593−601.
(6) Gestwicki, J. E.; Cairo, C. W.; Strong, L. E.; Oetjen, K. A.; Kiessling, L. L. Influencing Receptor−Ligand Binding Mechanisms with Multivalent Ligand Architecture. *J. Am. Chem. Soc.* **2002**, *124*, 14922−14933.
(7) Hartmann, M.; Lindhorst, T. K. The Bacterial Lectin FimH, a Target for Drug Discovery—Carbohydrate Inhibitors of Type 1 Fimbriae-Mediated Bacterial Adhesion. *Chem.—Eur. J.* **2011**, *2011*, 3583−3609.
(8) Ashton, P. R.; Boyd, S. E.; Brown, C. L.; Nepogodiev, S. A.; Meijer, E. W.; Peerlings, H. W. I.; Peerlings, H. W. I.; Stoddart, J. F. Synthesis of Glycodendrimers by Modification of Poly(propylene imine) Dendrimers. *Chem.—Eur. J.* **1997**, *3*, 974−984.
(9) Lindhorst, T.; Kieburg, C.; Krallmann-Wenzel, U. Inhibition of the Type 1 Fimbriae-Mediated Adhesion of *Escherichia coli* to Erythrocytes by Multiantennary α-Mannosyl Clusters: The Effect of Multivalency. *Glycoconjugate J.* **1998**, *15*, 605−613.
(10) de la Fuente, J. M.; Barrientos, A. G.; Rojas, T. C.; Rojo, J.; Cañada, J.; Fernández, A.; Penadés, S. Gold Glyconanoparticles As Water-Soluble Polyvalent Models to Study Carbohydrate Interactions. *Angew. Chem., Int. Ed.* **2001**, *40*, 2257−2261.
(11) Lin, C.-C.; Yeh, Y.-C.; Yang, C.-Y.; Chen, C.-L.; Chen, G.-F.; Chen, C.-C.; Wu, Y.-C. Selective Binding of Mannose-Encapsulated Gold Nanoparticles to Type 1 Pili in *Escherichia coli*. *J. Am. Chem. Soc.* **2002**, *124*, 3508−3509.
(12) Fulton, D. A.; Stoddart, J. F. Neoglycoconjugates Based on Cyclodextrins and Calixarenes. *Bioconjugate Chem.* **2001**, *12*, 655−672.
(13) Disney, M. D.; Zheng, J.; Swager, T. M.; Seeberger, P. H. Detection of Bacteria with Carbohydrate-Functionalized Fluorescent Polymers. *J. Am. Chem. Soc.* **2004**, *126*, 13343−13346.
(14) Tian, X.; Pai, J.; Baek, K. H.; Ko, S. K.; Shin, I. Fluorophore-Labeled, Peptide-Based Glycoclusters: Synthesis, Binding Properties for Lectins, and Detection of Carbohydrate-Binding Proteins in Cells. *Chem.—Asian J.* **2011**, *6*, 2107−2113.
(15) Durka, M.; Buffet, K.; Iehl, J.; Holler, M.; Nierengarten, J. F.; Vincent, S. P. The Inhibition of Liposaccharide Heptosyltransferase WaaC with Multivalent Glycosylated Fullerenes: A New Mode of Glycosyltransferase Iinhibition. *Chem.—Eur. J.* **2012**, *18*, 641−651.
(16) Wang, K.-R.; Wang, Y.-Q.; An, H.-W.; Zhang, J.-C.; Li, X.-L. A Triazatruxene-Based Glycocluster as a Fluorescent Sensor for Concanavalin A. *Chem.—Eur. J.* **2013**, *19*, 2903−2909.
(17) Weber, T.; Chandrasekaran, V.; Stamer, I.; Thygesen, M. B.; Terfort, A.; Lindhorst, T. K. Switching of Bacterial Adhesion to a Glycosylated Surface by Reversible Reorientation of the Carbohydrate Ligand. *Angew. Chem., Int. Ed.* **2014**, *53*, 14583−14586.
(18) Barnard, A.; Smith, D. K. Self-Assembled Multivalency: Dynamic Ligand Arrays for High-Affinity Binding. *Angew. Chem., Int. Ed.* **2012**, *51*, 6572−6581.
(19) Lim, Y. B.; Lee, M. Self-Assembled Multivalent Carbohydrate Ligands. *Org. Biomol. Chem.* **2007**, *5*, 401−405.
(20) Belitsky, J. M.; Nelson, A.; Hernandez, J. D.; Baum, L. G.; Stoddart, J. F. Multivalent Interactions between Lectins and

DOI: 10.1021/acsami.5b00702
ACS Appl. Mater. Interfaces 2015, 7, 7351−7356

Supramolecular Complexes: Galectin-1 and Self-Assembled Pseudopolyrotaxanes. *Chem. Biol.* **2007**, *14*, 1140−1151.
(21) Müller, M. K.; Brunsveld, L. A Supramolecular Polymer as a Self-Assembling Polyvalent Scaffold. *Angew. Chem., Int. Ed.* **2009**, *121*, 2965−2968.
(22) Yu, G.; Ma, Y.; Han, C.; Yao, Y.; Tang, G.; Mao, Z.; Gao, C.; Huang, F. A Sugar-Functionalized Amphiphilic Pillar[5]arene: Synthesis, Self-Assembly in Water, and Application in Bacterial Cell Agglutination. *J. Am. Chem. Soc.* **2013**, *135*, 10310−10313.
(23) Aldaye, F. A.; Palmer, A. L.; Sleiman, H. F. Assembling Materials with DNA as the Guide. *Science* **2008**, *321*, 1795−1799.
(24) Seeman, N. C. Nanomaterials Based on DNA. *Annu. Rev. Biochem.* **2010**, *79*, 65−87.
(25) Liu, D.; Cheng, E.; Yang, Z. DNA-Based Switchable Devices and Materials. *NPG Asia Mater.* **2011**, *3*, 109−114.
(26) Dong, Y.; Yang, Z.; Liu, D. DNA Nanotechnology Based on i-Motif Structures. *Acc. Chem. Res.* **2014**, *47*, 1853−1860.
(27) Kwak, M.; Herrmann, A. Nucleic Acid/Organic Polymer Hybrid Materials: Synthesis, Superstructures, and Applications. *Angew. Chem., Int. Ed.* **2010**, *49*, 8574−8587.
(28) Chien, M. P.; Rush, A. M.; Thompson, M. P.; Gianneschi, N. C. Programmable Shape-Shifting Micelles. *Angew. Chem., Int. Ed.* **2010**, *49*, 5076−5080.
(29) Edwardson, T. G. W.; Carneiro, K. M. M.; McLaughlin, C. K.; Serpell, C. J.; Sleiman, H. F. Site-Specific Positioning of Dendritic Alkyl Chains on DNA Cages Enables Their Geometry-Dependent Self-Assembly. *Nat. Chem.* **2013**, *5*, 868−875.
(30) Wang, L.; Feng, Y.; Sun, Y.; Li, Z.; Yang, Z.; He, Y.-M.; Fan, Q.-H.; Liu, D. Amphiphilic DNA-Dendron Hybrid: A New Building Block for Functional Assemblies. *Soft Matter* **2011**, *7*, 7187−7190.
(31) Wang, L.; Feng, Y.; Yang, Z.; He, Y. M.; Fan, Q.-H.; Liu, D. Reversibly Controlled Morphology Transformation of an Amphiphilic DNA-Dendron Hybrid. *Chem. Commun.* **2012**, *48*, 3715−3717.
(32) Zhao, Z.; Wang, L.; Liu, Y.; Yang, Z.; He, Y. M.; Li, Z.; Fan, Q.-H.; Liu, D. pH-Induced Morphology-Shifting of DNA-*b*-Poly(propylene oxide) Assemblies. *Chem. Commun.* **2012**, *48*, 9753−9755.
(33) Zhao, Z.; Wu, F.; Yang, Z.; Liu, D.; Fan, Q.-H. Synthesis and Self-Assembly of DNA-Aliphatic Polyether Dendron Hybrids. *Acta Chim. Sin.* **2013**, *71*, 549−554.
(34) Appeldoorn, C. C. M.; Joosten, J. A. F.; Ait el Maate, F.; Dobrindt, U.; Hacker, J.; Liskamp, R. M. J.; Khan, A. S.; Pieters, R. J. Novel Multivalent Mannose Compounds and Their Inhibition of the Adhesion of Type 1 Fimbriated Uropathogenic *E. coli*. *Tetrahedron: Asymmetry* **2005**, *16*, 361−372.
(35) Ella-Menye, J.-R.; Nie, X.; Wang, G. Synthesis of Octahydropyrano[3,2-*b*]pyrrole-2-carboxylic Acid Derivatives from D-Mannose. *Carbohydr. Res.* **2008**, *343*, 1743−1753.
(36) Spinelli, N.; Defrancq, E.; Morvan, F. Glycoclusters on Oligonucleotide and PNA Scaffolds: Synthesis and Applications. *Chem. Soc. Rev.* **2013**, *42*, 4557−4573.
(37) Li, Z.; Zhang, Y.; Fullhart, P.; Mirkin, C. A. Reversible and Chemically Programmable Micelle Assembly with DNA Block-Copolymer Amphiphiles. *Nano Lett.* **2004**, *4*, 1055−1058.
(38) Alemdaroglu, F. E.; Ding, K.; Berger, R.; Herrmann, A. DNA-Templated Synthesis in Three Dimensions: Introducing a Micellar Scaffold for Organic Reactions. *Angew. Chem., Int. Ed.* **2006**, *45*, 4206−4210.
(39) de Vries, J. W.; Zhang, F.; Herrmann, A. Drug Delivery Systems Based on Nucleic Acid Nanostructures. *J. Controlled Release* **2013**, *172*, 467−483.
(40) Dong, Y.; Liu, D.; Yang, Z. A Brief Review of Methods for Terminal Functionalization of DNA. *Methods* **2014**, *67*, 116−122.

DOI: 10.1021/acsami.5b00702
ACS Appl. Mater. Interfaces 2015, 7, 7351−7356